Effect of kaolin and argillite mixtures on the dielectric properties of geopolymers

S. Petlitckaia, A. Gharzouni, I.N. Vlasceanu, O. Tantot, I. Sobrados, A. Piancastelli, S. Rossignol

Effect of kaolin and argillite mixtures on the dielectric properties of geopolymers

S. Petlitckaia[1], A. Gharzouni[1], I.N Vlasceanu[1], O. Tantot[2], I. Sobrados[3], A. Piancastelli[4], S. Rossignol [1].

[1] IRCER: Institut de Recherche sur les Céramiques (UMR7315), 12 rue Atlantis, 87068 Limoges, France.

[2] XLIM, UMR CNRS 7252, Avenue Albert Thomas, 87000 Limoges, France

[3]Instituto de Ciencia de Materiales de Madrid, Consejo Superior de Investigaciones Científicas (CSIC), C/Sor Juana Inés de la Cruz, 3, 28049 Madrid, Spain

[4] CNR – Instituto di Scienza e Tecnologia dei Material Ceramici, 64 via Granaralo, I-48018 Faenza, Italy

■ Corresponding author: sylvie.rossignol@unilim.fr, tel.: 33 5 87 50 25 64.

Abstract

The use of geopolymer in radiofrequency applications and more precisely in antenna is innovative. The objective of this study is to highlight the impact of mixtures of kaolin and argillite on the structure and dielectric properties of geopolymers for antenna application. For this, six geopolymer formulations based on mixtures of kaolin and argillite with different proportions (33, 50 and 67 %) and calcined at 600 and 750 °C were studied using mercury intrusion porosimetry, dielectric measurements and NMR spectroscopy. Low porosity values were obtained whatever the mixture. At 600°C, the porosity increases with the increase of argillite content from 18 to 23%. At 750°C, no impact of argillite content on the porosity (16%) was detected. However, the pore size increases with increasing the argillite content regardless of the calcination temperatures due to the unreacted secondary phases present in argillite. MAS-NMR experiments on geopolymer samples and calcined mixtures have evidenced a strong correlation between reactive aluminum resulting from dehydroxylation of

kaolin and clay minerals of argillite and the geopolymerization rate. These structural variations influence the dielectric properties. Indeed, ε and tan δ values increase with the increase of argillite content and calcination temperature due to the increase in the number of moles of free alkali earth cations (Ca^{2+} and Mg^{2+}).

Keywords: geopolymers, dielectric properties, MAS-NMR, porosity, carbonates

I. Introduction

Geopolymers are amorphous three-dimensional mineral binders, obtained by the activation of an aluminosilicate source by an alkaline solution at low temperature [1, 2]. A multitude of raw materials such as metakaolins, clays, fly ash, slag, red mud, waste glass or the mixture of these materials can be used for synthesis geopolymers [3, 4]. The properties of raw materials strongly influence the structure and the properties of the final materials. Autef et al., [5] have demonstrated the importance of metakaolin properties such as the wettability, the amorphous phase and the dehydroxylation extent on the structure and the mechanical properties of geopolymer .The influence of calcium on the properties of geopolymer was also investigated. It was shown that it strongly depends on the content, the form and the source of calcium [6]. In fact, calcium can precipitates as portlandite $Ca(OH)_2$ or reacts with silicate and aluminates [6, 7,]. Addition of calcium compounds such as CaO and $Ca(OH)_2$ improves the mechanical properties of the fly ash based geopolymers [8]. Dupuy et al., [9] have demonstrated that the geopolymerization reaction and the mechanical strengths of Callovo-Oxfordian (COx) argillite based materials depends not only on the reactive aluminium but also on carbonate species evolution after alkali activation. The effect of calcium on geopolymer porosity was also highlighted. For example, the replacement of fly ash by blast furnace slag i.e. the increase of calcium content leads to the decrease of the porosity and the pore size distribution is shifted to micro-porosity [10,11]. Other studies have focused on the influence of calcium on the thermal properties. It was demonstrated that the calcium content

and availability impact the phase transformation at high temperatures, and the strength after thermal treatment [12]. Geopolymers based on calcined mixtures of kaolin and argillite were also characterized by a thermal resistance at 1000°C and an improvement in mechanical strength especially for the mixture composed of 67% argillite. This result was explained by in situ formation of thermally resistant crystalline phases such as wollastonite [13]. The impact of carbonates on the geopolymerization reaction will also impact other working properties such as dielectric one. In fact, dielectric properties of geopolymer are recently gaining increasing interest [14,15]. The investigation of dielectric properties of geopolymer is interesting since they can be used in radiofrequency applications and more precisely as matrix in antenna to replace currently used resin [15]. In fact, the use of geopolymer will permit on one hand the miniaturization of wideband antennas which is necessary to obtain compact devices such as wearable and/or disposable ones [16]. On the other hand, the use of inorganic materials is more eco-friendly and less pollutant.

Some studies have investigated fresh and aged fly ash based geopolymers. They have found that the dielectric properties depend on many factors such as the frequency, the alkali cation concentration [17], the reaction rate [18], the porosity and the density of the geopolymer [19] and the water content [20]. In fact, the dielectric properties of geopolymers (ε and tan δ) were demonstrated to increase with the increase of free water amount. This fact was explained by the easy polarization of H–O–H bonds by an electric field. Water will also permit the movement of free alkali cation along the pore increasing consequently the ionic electrical conductivity of geopolymer materials [21]. Other authors have studied the dielectric properties of acid based geopolymer [22,23]. They have found that that dielectric values increased with the decrease of Si/P molar ratio due to enhancement of ionic conduction. It was also highlighted that acid based geopolymer permits also to decrease the dielectric loss compared to alkali based one because the ion transfer is negligible [24]. Thus, the effect of

different raw materials with complex mineralogy and especially the effect of carbonate and the final structure of geopolymer on the dielectric properties is not yet fully understood.

The objective of the present work is to study the influence of calcined mixture of kaolin and argillite at two different temperatures on the porosity, structure and dielectric properties of the resulting geopolymers. The variation of the argillite content in the mixture and the calcination temperature will modify the calcium and aluminium content availability and reactivity. The novelty of the study consists on the evaluation of dielectric properties of kaolin and argillite mixtures based geopolymers for antenna applications and to determine the factors controlling these properties.

For this purpose, several characterization were carried on such as mercury intrusion porosimetry, NMR spectroscopy and dielectric measurements.

II. Experimental part

Raw materials and sample preparation

The samples are prepared using two aluminosilicate sources such as kaolin that contains traces of calcite [25] and Callovo-Oxfordian argillite [26]. Kaolin was mixed with the argillite with different mass proportions and calcined at 600 or 750°C. The Chemical and physical characteristics of the aluminosilicate sources used are detailed in previous work [13]. The adopted nomenclature is Y and Y' for the mixtures calcined at 600 and 750°C, respectively with Y=A, B, C and Y' = A', B', C' with (A, A'), (B, B') and (C, C') contain 33, 50 and 67 wt.% of argillite. These mixtures are mixed with an alkaline silicate solution (Si/K = 0.58) under strong mixing for 5 min. Samples are casted in closed molds and stored at room temperature for seven days. The geopolymer samples are named GY and GY' as detailed in **Table 1.**

Characterization techniques

Differential and thermogravimetric (DTA-TGA) thermal analysis were performed for the mixtures of raw materials with a TA Instrument SDT Q600. The samples were placed in platinum crucibles. The measurement was carried out in atmosphere of dry air (100 mL/min) between 30 and 1000 °C with a rate of 10 °C/min.

The pores size distribution in the range 0.0078 - 100 µm was analyzed by mercury porosimetry (surface tension = 0.48 N/m and contact angle =140 °, Thermo Finnigan Pascal 140 and Thermo Finnigan Pascal 240). The measurement were performed on monolith sample, with an experimental error of 4 % due to the accuracy of the instrument.

High-resolution NMR experiments were performed on aluminosilicate mixtures and consolidated geopolymers at room temperature using a Bruker AVANCE-400 spectrometer, operating at 104.26 MHz for ^{27}Al signal and 79.49 MHz for ^{29}Si signal. The powders were deposited in a zirconia rotor (Ø = 4 mm). The spinning rate was 10 kHz. The ^{27}Al (I = 5/2) MAS NMR spectra were recorded after p/8 pulse irradiation (1.5 µs) using a 1- MHz filter to improve the signal/noise ratio. A solution of $AlCl_3$ was used as a reference. The ^{29}Si (I = 1/2) MAS NMR spectra were recorded after a π/2-pulse irradiation (4 µs) using a 500 kHz filter to improve the signal/noise ratio. In each case, 400 scans were collected. The time between acquisitions was set to 10 s to minimize saturation effects. Tetramethylsilane (TMS) was used as a reference standard. The estimated errors for chemical shifts and relative area are estimated of 1 ppm and 2% respectively. The fitting of NMR spectra was performed with the Winfit program (Bruker).

Dielectric measurements were effectuated using the VNA Keysight E5063A which provided high-precision dielectric parameter measurements (permittivity, permeability and loss tangent). For samples homogeneous measurements and characterization, the loaded rectangular waveguide method was chosen despite its reduced frequency band in mono mode (fcTE10 = 1.735 GHz and fcTE20 = 3.47 GHz for WR340 standard of this study). To

duplicate the means of multi-site characterization and ensure a good level of adaptation, it was decided to carry out the transitions from the coaxial guide to the rectangular one. The guiding idea of the design is to facilitate the casting of geopolymers in the sample holder and improve its performance in terms of adaptation of the order of 25 dB between 2 and 3.3 GHz. TRL calibration resulted in a measurement error of |Sij] 0.03 dB and arg(Sij) 0.4°. The geopolymer samples were previously dried at 90°C. Humidity affects the dielectric properties (permittivity and loss tangent) of geopolymers. This behavior has been previously observed and was attributed to water and cation mobility in the geopolymer [16, 27]. Measurements of standard samples (plexiglass and Teflon) were made and comparisons of complex permittivity extracted by NRW algorithm and by another free space method have shown good agreements and validated the whole process. The sample is connected by a phase and amplitude stable cable to a VNA which is then calibrated with thru, reflect and line for WR340.

III. Results and discussion

In order to assess the effect of carbonate and reactive aluminium, the argillite content in the initial mixture (33, 50 and 67%) and calcination temperature (600 and 750°C) were varied and their effect on the porosity and structure of the resulting geopolymer as well as their dielectric properties, was investigated.

1) Porosity and structure

Table 2 reports the main results of apparent density, surface area, porosity, pore volume and average pore diameter determined by mercury intrusion porosimetry. The data show that the apparent density is quite similar for all samples and is in the range of 2.24 - 2.40 g/cm^3. These values are in accordance with literature [28,29]. Specific surface area of geopolymer materials decreases with increasing the argillite content for both calcination temperatures of the raw mixtures (from 20 to 12 m^2/g for GA and GC, respectively and from 21 to 9 m^2/g for

GA' and GC', respectively). The obtained specific surface values are lower than those of metakaolin and potassium-based geopolymer (about 155 m^2/g) [3, 30] and similar to fly ash based one (about 8 m^2/g) [31]. Furthermore, whatever the sample, the porosity value ranges from 16 to 23 % which is lower than the value obtained for geopolymers usually varying between 30 and 50 % depending the used aluminosilicate source (metakaolin or fly ash) and alkaline solution (potassium or sodium) [32,33,34]. The lower obtained values are due to the use of argillite. Indeed, Dupuy et al., [35] have shown a low porosity varying from 18 to 23% for argillite based geopolymers. At 600°C, the porosity decreases with the increase of the argillite content from 33 to 50% (18 and 14% for GA and GB, respectively) and then increases at 67% of argillite (23%).The difference for GB is due to carbonates compounds promoting the solid reaction between the various species [34]. At 750°C, the porosity value of GA', GB' and GC' samples is about 16 % whatever the argillite content. The pore volume follows the same trend as for the porosity. This result reveals that more reaction products i.e geopolymer network are formed for materials based on mixtures calcined at 750°C which reduce the porosity [20]. The pore size distribution is shown in **Figure 1**. The pore size distribution is monomodal in the range 0.01-0.025 µm and 0.01-0.03 µm for GA and GB samples respectively. The same type of distribution (monomodal) was observed for GA' and GB' samples with a pore size in the range 0.01-0.02 µm. In the case of GC and GC' samples, the pore size distribution becomes bimodal, with the first peak detected at 0.03 µm and the second at 1µm and 0.4 µm. Data indicate that the average pore diameter increases with increasing the argillite content for both calcination temperatures. This fact can be explained by the unreacted secondary phases present in argillite such as muscovite, calcite and quartz [10,13], inducing heterogeneity of the microstructure and therefore higher pore size [36]. Consequently, the porosity and pore size distribution are highly dependent on the chemical composition and the thermal history of the used aluminosilicate source. For further structural

informations, ^{27}Al and ^{29}Si MAS-NMR experiments were performed on geopolymer samples **(Figure 2 A,B)**. An example of deconvoluted spectrum of GA sample is presented in **Figure 2A**. Deconvolution details are reported in **Table 3**. Irrespective of the sample, the spectra are typical of geopolymer materials [37]. Indeed, a dominant phase at approximately 58 ppm, attributed to four-coordinated aluminium ($Al^{(IV)}$) is observed and denotes the formation of the geopolymer network. A minor broad peak centered at about 3 ppm, corresponding to six-coordinated aluminium $Al^{(VI)}$ is attributed to non-reacted species [38]. With the increase of argillite proportion in the mixture, the percentage of $Al^{(VI)}$ increases in detriment of $Al^{(IV)}$ from 3.4 to 7.7 % for GA and GC and from 2.2 to 6.3 % for GA' and GC' respectively. This fact can be explained by higher reactivity of metakaolin compared argillite (more rapid dissolution). Small differences can be detected at 750°C **(Figure 2B)** i.e a slight increase of four-coordinated aluminium compared to samples based on mixtures calcined at 600°C. More informations can be provided by ^{29}Si MAS-NMR **(Figure 2 C,D)**. The adopted nomenclature is $Q^n(mAl)$ with n is the polymerization degree of the silicon tetrahedra and m the amount of aluminium substitution per silicon tetrahedron [39]. Broad signal revealing a disordered structure is obtained whatever the sample [40]. Five components at about -84,-89, -94, -99 and -108 ppm (± 1 ppm) assigned to $Q^4(4Al)$, $Q^4(3Al)$, $Q^4(2Al)$, $Q^4(1Al)$ and $Q^4(0Al)$ contributions respectively and typical of three-dimensional structure of geopolymer materials [41, 42]. The latter contribution (at -108 ppm is attributed to quartz [32] initially present in kaolin and especially in argillite. Additional peaks at -75 and -80 ppm were also detected. Mackenzie et al [43] have found similar peaks in pyrophyllite based geopolymers and explain that by the retention of the crystalline 2:1 layer structure which resists to alkaline attack. This is also the case for 2:1 clays minerals originating from argillite. According to Davidovits [44], these peaks can be attributed to nesosilicates (Q^0 and Q^1) resulting from unreacted alkaline silicate solution. Whatever the sample, Q^4 (3Al) and Q^4 (2Al) (at around -89 and -94 ppm and

respectively) are the dominant contributions. At 600°C **(Figure 2A)**, A and B spectra exhibit quite similar contribution areas. However, B shows the highest Q^4(3Al) contribution percentage (29.7, 33.5 and 27.0 % for A, B and C samples, respectively). C spectrum is different from the two other samples showing the highest Q^4(2Al) contribution percentage (21.0, 22.9 and 29.3 % for A, B and C samples, respectively) and slightly shifted to -92.2 ppm. This is may be due the presence of another contribution due to argillite at the same chemical shift which is Q^3(0Al) generally detected at -93 ppm in the illite-smectite clays [45].

At 750°C **(Figure 2B)**, the spectra are quite similar. Q^4(3Al) is the major contribution whatever the sample revealing a higher aluminium incorporation in the framework [46, 47]. This fact reveals higher reaction extent due to higher reactive aluminum resulting from dehydroxylation of kaolin and clay minerals of argillite. In order to highlight the role of the raw mixtures (argillite and kaolin) on the final structure of geopolymers, they were analyzed by ^{27}Al MAS-NMR spectroscopy after thermal treatment at 600 and 750°C **(Figure 2E, F)**. An example of deconvolution of the obtained spectrum of A mixture is presented in **Figure 2Ea**. Data concerning the chemical shifts and the percentages of the curve area of the various contributions are given in **Table 3**. Three environments of aluminium can be noticed. Spinning sidebands are also observed due to the presence of hematite in a major part from argillite and a in minor part from kaolin [26,48,49]. The 6-coordinated aluminium (Al^{VI}) can be detected by the components at 13.5, 2.8 and -6 ppm and exhibits the highest percentage of 42%. It corresponds to aluminum present in smectite, illite and micas from argillite [2] and impurities of kaolin [21]. The 5-coordinated aluminium (Al^{V}) is detected at 28 ppm with percentage of 31 % and is due to the dehydroxylation of kaolinite [19, 50]. The 4- coordinated aluminium (Al^{IV}) at 48.5, 57 and 65 ppm presents the lowest percentage of about 27% due the beginning of dehydroxylation of the 2:1 clay minerals of argillite characterized by direct formation of Al^{IV} from initial Al^{VI} without formation of Al^{V} [22]. With the increase of argillite

content, the percentage of 6-coordinated aluminum increases to 39 and 51% for B and C mixtures, respectively. The 5-coordinated aluminium percentage decreases to 27 and 16% for B and C samples respectively. The tetrahedral aluminum is about 35 and 33% for B and C samples respectively. At 750 °C, the Al^{VI} and Al^{V} percentages decrease drastically in detriment of the increase of Al^{IV} (30, 44 and 56% for A', B' and C' mixtures, respectively) revealing complete dehydroxylation of the clay minerals of the argillite [51]. In order to correlate the structure of final materials with the characteristics of raw materials, the evolution of the contributions area ratio $\frac{Q^4\,(3Al)}{\sum Q^4\,(nAl)}$ with n= 0, 1, 2 and 4 of geopolymer samples, indicating the formation rate of geopolymer in function of the $\frac{Al^{IV}+\,Al^{V}}{Al^{VI}}$ characteristic of the reactive aluminium was plotted in **Figure 3**. The $\frac{Q^4\,(3Al)}{\sum Q^4\,(nAl)}$ ratio increases with the increase of $\frac{Al^{IV}+\,Al^{V}}{Al^{VI}}$ ratio. At 750°C, the dehydroxylation of clay minerals is enhanced favoring the formation of reactive aluminium ($Al^{V}+\,Al^{IV}$) which reacts to form the geopolymer network.

Consequently, the major formed network is dependent on the argillite content and calcination temperature. The detected structural variation will influence the working properties.

2) Dielectric properties

Figure 4 shows an example of dielectric and magnetic measurements of GA sample between 2 and 3.3 GHz. The values of the real part of dielectric constant indicates the ability of the material to store microwave energy and dielectric loss quantifies a dielectric material's inherent dissipation of electromagnetic energy. Permeability is the ability to support formation of magnetic fields in a material. The values of ε for frequencies between 2 and 3.3 GHz for this composition were around 3.5, while tan δ values were around 0.05. The values of μ for same range of frequency was around 1, because of no magnetic addition. These values

are in agreement with previous works [16, 23]. The obtained values of permittivity (ε), tan δ and permeability (μ) at 2.45 GHz (T = 20°C, 40-50 % HR) for the different studied samples are reported in **Table 4.** Samples calcined at 600˚C presented ε values of 3.59, 3.69 and 3.68 and tan δ values of 0.051, 0.038 and 0.034, for 33, 50 and 67% of argillite respectively. For samples calcined at 750˚C, higher ε and tan δ values were obtained (about 3.81, 4.05 and 4.20 and 0.064, 0.061 and 0.095 for samples based on 33, 50 and 67 % argillite respectively). Thus, increasing the argillite content and the calcination temperature of kaolin-argillite mixture induces an increase of dielectric values. This fact suggests that the higher content of calcium after carbonate decomposition at 750°C permits to increase the permittivity value. Similar results were obtained on $PbTiO_3$ ceramics showing the increase of dielectric constant with the increase of amount of calcium [52]. Concerning the permeability values, all samples showed values around 1, due to no magnetic addition [53].

In order to correlate the dielectric properties with the porosity results presented above, **Figure 5 (A, B**) presents the surface area and average pore diameter in function of ε value. Generally, the surface area decreases with the increase of ε value. At 600°C, as the argillite content increases, the decrease of the surface area is accompanied by a slight increase of ε value. However, at 750°C, the increase of ε is more pronounced. In contrary, the average pore diameter increases when ε increases and it is more noticeable for GA', GB', GC' samples. This fact indicates the crucial impact of calcination temperature of the raw mixture varying the carbonate decomposition.

In order to correlate the dielectric properties to the structural characteristics of the raw mixtures, the variation of ε values was plotted in function of the reactive aluminium $\frac{Al^{IV}+ Al^{V}}{Al^{VI}}$ (**Figure 6A)** and in function of the number of moles of free M^{2+} (M=Mg and Ca) determined from DTA-DTG on calcined mixtures at 600 and 750°C (see the supplementary file) in (**Figure 6B**). A linear correlation has been proven (R^2=0.92) showing the increase of ε values

with the increase of $\frac{Al^{IV}+Al^{V}}{Al^{VI}}$ ratio. At 600°C, the low value of $\frac{Al^{IV}+Al^{V}}{Al^{VI}}$ ratio (low $Al^{IV}+Al^{V}$) varying between 0.96 and 1.6 due to the low dehydroxylation extent of clay minerals leads to low value of ε varying very slightly in function of the argillite content (about 3.65). The variation of ε is more visible at 750°C (from 3.8 to 4.2) and this is seems to be related to the higher dehydroxylation extent of clay minerals leading to higher reactive aluminium (high $Al^{IV}+Al^{V}$). A linear correlation was also found between ε value and the number of moles of free M^{2+} (R^2=0.97). In fact, it is shown that ε increases with increasing M^{2+} which is higher with the increase of the argillite content and the calcination temperature. In fact the presence of free M^{2+} (Ca^{2+} and Mg^{2+}) which are not integrated into the geopolymer network will increase the conductivity of the material and therefore the increase of ε value [18]. Consequently, the dielectric properties are highly dependent on the chemical composition of raw mixture i.e. the argillite content and the calcination temperature which control the mineral clays dehydroxylation and the carbonates decomposition.

IV. Conclusion

Geopolymer formulations based on mixtures of kaolin and argillite with different proportions (33, 50 and 67 %) and calcined at 600 and 750 °C were studied. These temperatures were chosen to conserve or decompose the carbonates species initially present in argillite. It was demonstrated that the structure of the obtained geopolymers depends on the argillite content and the calcination temperature. Indeed, the formation of geopolymer network is favored by the increase of calcination temperature due to higher dehydroxylation extent of clay minerals and hindered with the increase of argillite content due to presence of impurities. These structural variations impact the porosity and the dielectric properties of the geopolymers. In fact, the porosity increases with the increase of argillite content (from 18 to 23%) when the raw mixtures are calcined at 600°C. However, the increase of the calcination temperature to 750°C, does not influence the porosity (17%). The pore size increases with

increasing the argillite content regardless of the calcination temperatures due to the unreacted secondary phases present in argillite. Concerning the dielectric properties, ε and tan δ values increase with the increase of argillite content and the calcination temperature due to the increase of free alkali earth cations (Ca^{2+} and Mg^{2+}). Thus, the obtained materials are suitable to be used in antenna. Depending on the desired dielectric properties, it is necessary to adapt the percentage of argillite in the mixture as well as the calcination temperature.

Acknowledgements

Project supported by Andra under the "Investing in the Future Programme" ("Investissement d'Avenir") - Selected under the Andra Call for Projects: "Optimisation of post-dismantling radioactive waste management", organized in cooperation with the French National Research Agency (ANR). NMR measurements were supported by Spanish ministry grant No. MAT2016-78362-C4-2R.

References

[1] J. Davidovits, Geopolymers, inorganic polymeric new materials. J. Therm. Anal. Calorim. 37 (1991) 1633-1656.

[2] P. Duxson, The structure and thermal evolution of metakaolin geopolymers. PhD thesis, University of Melbourne, 2006, pp.355

[3] X. Yao, Z. Zhang, H. Zhu, Y. Chen, Geopolymerization process of alkali-metakaolinite characterized by isothermal calrimetry. Thermochim. Acta. 493 (2009) 49-54.

[4] A. Buchwald, M. Hohman, K. Posern, E. Brendler, The suitability of thermally activated illite-smectite clay as raw material for geopolymer binders. Appl. Clay Sci. 46 (2009) 300-304.

[5] A. Autef, E. Joussein, G. Gasgnier, S. Pronier, I. Sobrados, J. Sanz, S. Rossignol, Role of metakaolin dehydroxylation in geopolymer synthesis, Powder Technol. 250 (2013) 33-39.

[6] C.K. Yip, G.C. Lukey, J. L. Provis, J. S.J. van Deventer, Effect of calcium silicate sources on geopolymerisation, Cem. Concr. Res. 38 (2008) 554-564.

[7] G. Lodeiro, A. Palomo, A. Fernández-Jiménez, D.E. Macphee Compatibility studies between N-A-S-H and C-A-S-H gels. Study in the ternary diagram Na_2O–CaO–Al_2O_3–SiO_2–H_2O I, Cem. Concr. Res. 41 (2011) 923-931.

[8] J. Temuujin, A. van Riessen, R. Williams, Influence of calcium compounds on the mechanical properties of fly ash geopolymer pastes, J. Hazard. Mater. 167 (2009) 82-88.

[9] C. Dupuy, A.Gharzouni, N. Texier-Mandoki, X. Bourbon, S. Rossignol, Alkali-activated materials based on callovo-oxfordian argillite: Formation, structure and mechanical properties, J. Ceram. Sci. Technol. 9(2) (2018) 127-140.

[10] Z. Li, S. Liu, Influence of Slag as Additive on Compressive Strength of Fly Ash-Based Geopolymer. J. Mater. Civil. Eng. 19 (2007) 470-474.

[11] Y. Luna-Galianoa, C. Fernández-Pereira, M. Izquierdo, Contributions to the study of porosity in fly ash-based geopolymers. Relationship between degree of reaction, porosity and compressive strength, Mater. Construc. 66 (2016) e098.

[12] K. Dombrowski, A.Buchwald, M. Weil, The influence of calcium content on the structure and thermal performance of fly ash based geopolymers. J. Mater. Sci. 42 (2007) 3033–3043.

[13] M.Tognonvi, S. Petlitckaia, A.Gharzouni, M.Fricheteau, N. Texier-Mandoki, X. Bourbon, S. Rossignol, High-temperature, resistant, argillite based, alkali activated materials with improved post-thermal treatment mechanical strength. Clays Clay Miner. 68 (2020) 211–219.

[14] H. Nadir, A. Gharzouni, E. Martinod, N. Feix, O. Tantot, V. Bertrand, S. Rossignol, M. Lalande, Design of UWB Antennas Integrating Geopolymer Material, 12th European Conference on Antennas and Propagation, 2018, https://doi.org/10.1049/cp.2018.1129

[15] N. Essaidi, H. Nadir, E. Martinod, N. Feix, V. Bertrand, O. Tantot, M. Lalande, S. Rossignol, Comparative study of dielectric properties of geopolymer matrices using different dielectric powders , J. Eur. Ceram. Soc. 37 (2017) 3551-3557.

[16] I.N. Vlasceanu, A. Gharzouni, O. Tantot, M. Lalande, C. Elissalde, S. Rossignol, Geopolymer as dielectric materials for ultra-wideband antenna applications: Impact of magnetite addition and humidity, Open Ceramics. 2 (2020) 100013.

[17] S. Hanjitsuwan, S. Hunpratub, P. Thongbai, S. Maensiri, V. Sata, P. Chindaprasirt, Effects of NaOH concentrations on physical and electrical properties of high calcium fly ash geopolymer paste, Cem. Concr. Compos. 45 (2014) 9-14.

[18] S. Zeng, J. Wang, Characterization of mechanical and electric properties of geopolymers synthesized using four locally available fly ashes, Constr. Build. Mater. 121 (2016) 386-399.

[19] A.B. Malkawi, H. Al-Mattarneh, B.E. Achara, B.S. Mohammed, M.F. Nuruddin, Dielectric properties for characterization of fly ash-based geopolymer binders, Constr. Build. Mater. 189, (2018) 19-32.

[20] S. Jumrat, B. Chatveera, P. Rattanadecho, Dielectric properties and temperature profile of fly ash-based geopolymer mortar, International Communications in Heat and Mass Transfer, 38 (2011) 242-248.

[21] X.M Cui, G.J Zheng, Y.C Han, F. Su, Ji. Zhou, A study on electrical conductivity of chemosynthetic Al_2O_3–$2SiO_2$ geoploymer materials, J. Power Sources. 184 (2008) 652-656.

[22] H. Douiri, S. Louati, S. Baklouti, M. Arous, Z. Fakhfakh, Structural, thermal and dielectric properties of phosphoric acid-based geopolymers with different amounts of H_3PO_4, Mater. Lett. 116 (2014) 9-12.

[23] L.P. Liu, X.M. Cui, Y. He, J.L.Yu, Study on the dielectric properties of phosphoric acid-based geopolymers. Mater. Sci. Forum. 663-665 (2010) 538-541.

[24] X.M. Cui, L.P. Liu, Y. He, J.Y. Chen, J. Zhou, A novel aluminosilicate geopolymer materials with low dielectric loss, Mater. Chem. Phys. 130 (2011)1-4.

[25] A. Gharzouni, Contrôle de l'attaque des sources aluminosilicates par la compréhension des solutions alcalines. PhD. thesis, University of Limoges, France, 2016.

[26] A. Gharzouni, C. Dupuy, I. Sobrados, E. Joussein, N. Texier-Mandoki, X. Bourbon and S. Rossignol, The effect of furnace and flash heating on Cox argilite for the synthesis of alkali-activated binders, J. Clean. Prod. 156 (2017) 670-678.

[27] I.N. Vlasceanu, A. Gharouni, O. Tantot, E. Martinod, S. Rossignol, Geopolymer Carbon-Based for Ultra – Wideband Absorbent Applications, Molecules. 25 (2020) 4218

[28] F.G.M. Aredes, T.M.B. Campos, J.P.B. Machado, K.K. Sakane, G.P. Thim, D.D. Brunelli, Effect of cure temperature on the formation of metakaolinite-based geopolymer, Ceramic. Int. 41 (2015) 7302-7311.

[29] P. Steins, A. Poulesquen, F. Frizon, O. Diat, J. Jestin, J. Causse, D. Lambertin and S. Rossignol, Effect of aging and alkali activator on the porous structure of a geopolymers, J. Appl. Crystallogr. 47 (2014) 316-324.

[30] Q. H. Nguyen, S. Lorente, A. Duhart-Barone, H. Lamotte, Porous arrangement and transport properties of geopolymers, Constr. Build. Mater. 191 (2018) 853-865.

[31] S. Andini, R. Cioffi, F. Colangelo, T. Grieco, F. Montagnaro, L. Santoro, Coal fly ash as raw material for the manufacture of geopolymer-based products, J. Waste Manag. 28 (2008) 416-423.

[32] J.L Bell, W.M. Kriven, Nanoporosity in Aluminosilicate, Geopolymeric Cements, Microsc. Microanal. 10 (2004) 590-591.

[33] A. Fernandez-Jimenez, D.E. Macphee, E.E. Lachowski, A. Palomo, Immobilization of cesium in alkaline activated fly ash matrix. J. Nucl. Mater. 346 (2005) 185-193.

[34] F. Skvara, L. Kopecky, J. Nemecek, Z. Bittnar, Microstructure of geopolymer materials based on fly ash. Ceram. - Silik. 50 (2006) 208-215.

[35] C. Dupuy, A. Gharzouni, N. Texier-Mandoki, X. Bourbon, S. Rossignol, Thermal resistance of argillite-based alkali-activated materials. Part 1: Effect of calcination processes and alkali cation, Mater. Chem. Phys. 217 (2018) 323-333.

[36] P. Duxson, J.L. Provis, G.C. Lukey, S.W. Mallicoat, W.M. Kriven, J.S.J. VanDeventer, Understanding the relationship between geopolymer composition, microstructure and mechanical properties, Colloids Surfaces A Physicochem. Eng. Asp. 269 (2005) 47-58.

[37] R.A. Fletcher, K.J.D. MacKenzie, C.L. Nicholson, S.Shimada, The composition range of aluminosilicate geopolymers, J. Eur. Ceram. Soc. 25 (2005)1471-1477.

[38] J.V. Walther, Relation between rates of aluminosilicate mineral dissolution, pH, temperature, and surface charge Am. J. Sci. 7 (1996) 296-693,

[39] S.L.A. Valcke, P. Pipilikaki, H. R. Fischer, M. H.W. Verkuijlen, E.R.H. van Eck, FT-IR and ^{29}Si-NMR for evaluating aluminium–silicate precursors for geopolymers, Mater. Struct. 48 (2015) 557-569.

[40] C. Ferone, B. Liguori, I. Capasso, F. Colangelo, R. Cioffi, E. Cappelletto, R. Di Maggio,Thermally treated clay sediments as geopolymer source material, Appl. Clay Sci. 107 (2015) 195-204.

[41] P. Duxson, J.L. Provis, G.C. Lukey , F. Separovic and J.S.J. van Deventer, ^{29}Si NMR Study of Structural Ordering in Aluminosilicate Geopolymer Gels. Langmuir, 21 (2005) 3028–3036.

[42] J. Klinowski, Nuclear magnetic resonance studies of zeolites, Prog. Nucl. Mag. Res. Sp. 16 (1984) 237-309.

[43] K.J.D. MacKenzie, S. Komphanchai, R.Vagana, Formation of inorganic polymers (geopolymers) from 2:1 layer lattice aluminosilicates, J. Eur. Ceram. Soc. 28 (2008) 177-181.

[44] J. Davidovits, Geopolymer Chemistry and Applications, 2nd edition, 2008

[45] N. Garg, J. Skibsted, Pozzolanic reactivity of a calcined interstratified illite/smectite (70/30) clay, Cement Concrete Res. 79 (2016) 101-111

[46] S.K. Lee, J.F. Stebbins, The degree of aluminum avoidance in aluminosilicate glasses Am Miner. 84 (1999) 937-945.

[47] S.L.A. Valcke, P. Pipilikaki, H.R. Fischer, M. H. W. Verkuijlen et E. R. H. van Eck FT-IR and ^{29}Si-NMR for evaluating aluminium–silicate precursors for geopolymers. Mater. Struct. 48 (2015) 557–569 https://doi.org/10.1617/s11527-014-0432-2

[48] G. Thompson, 1984. 29Si and 27Al Nuclear Magnetic Resonance Spectroscopy of 2:1. Clays, Clay Miner. 19, 229-236.

[49] A. Gharzouni, I. Sobrados, E. Joussein, S. Baklouti, S. Rossignol, Control of polycondensation reaction generated from different metakaolins and alkaline solutions, J. Ceram. Sci. Technol 8 (2017) 365-376.

[50] J. Dietel, L. N. Warr, M. Bertmer, A. Steudel, G. H. Grathoff, K. Emmerich,The importance of specific surface area in the geopolymerization of heated illitic clay, Appl. Clay Sci. 139 (2017) 99-107.

[51] G.E. Roch, M.E. Smithi, S.R. Drachman, Solid state NMR Characterization of the thermal transformation of an illite-rich clay. Clays Clay Miner. 46 (1998) 694-704.

[52] S.Y. Chu, C.H Chen, Effect of calcium on the piezoelectric and dielectric properties of Sm-modified PbTiO3 ceramics, Sensors and Actuators A: Physical, 89, (2001) 210-214.

[53] Y. Zhang, P. He, J. Yuan, C. Yang, D. Jia, Y. Zhou, Effects of graphite on the mechanical and microwave absorption properties of geopolymer based composites, Ceramic. Int. 43 (2017) 2325-2332.

(A)

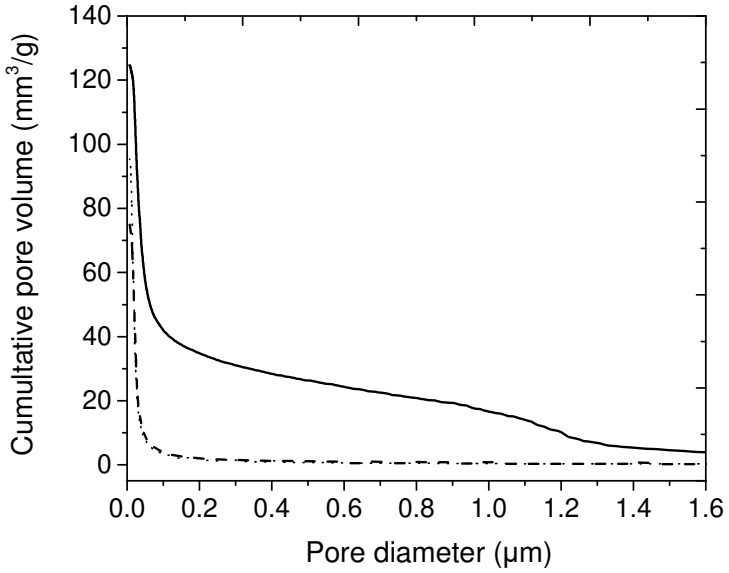

(B)

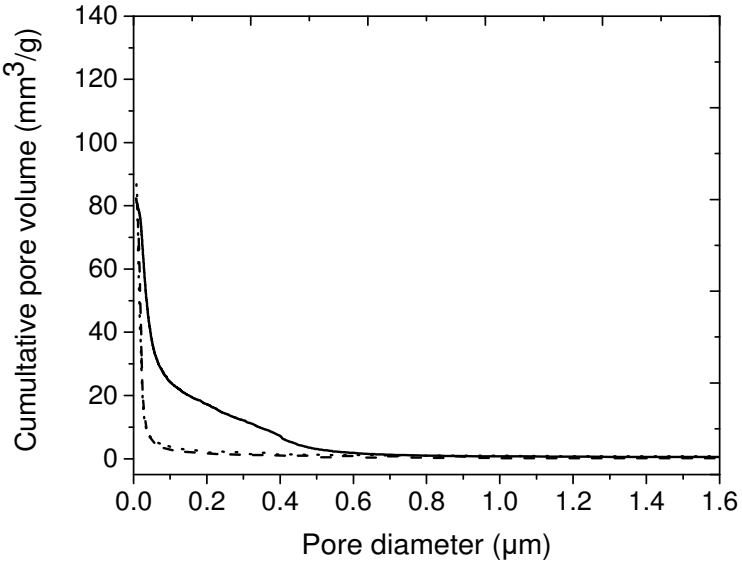

Figure 1 : The pore size distribution of (A) GY and (B) GY' geopolymers samples (where (…) A, A', (---) B, B' and (—) C, C').

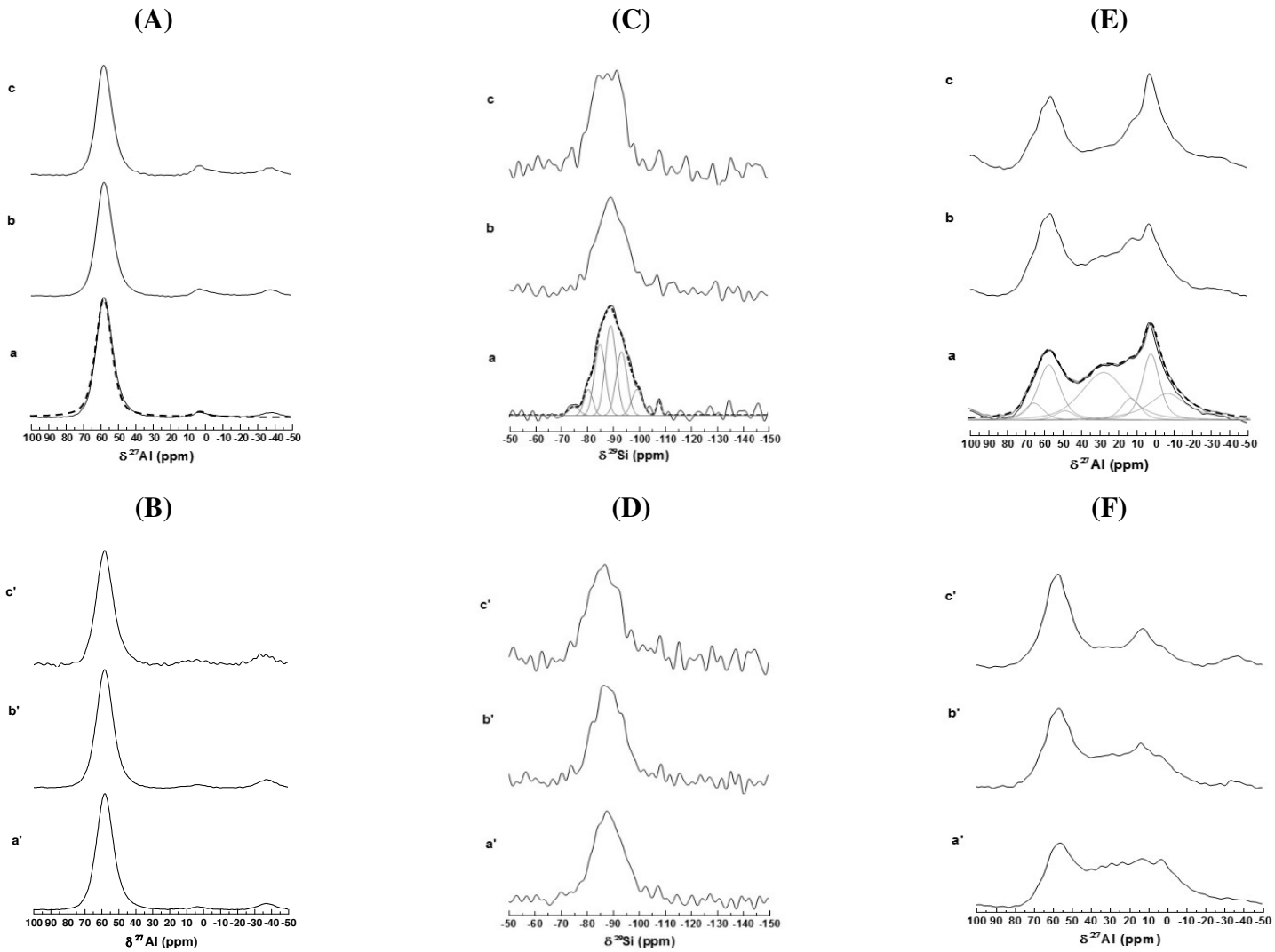

Figure 2: (A, B) ^{27}Al and **(C, D)** ^{29}Si MAS –NMR spectra of GY and GY' geopolymer samples and **(E, F)** ^{27}Al MAS –NMR of Y and Y' mixtures (where (a, a') A, A', (b, b') B, B' and (c, c') C,C')

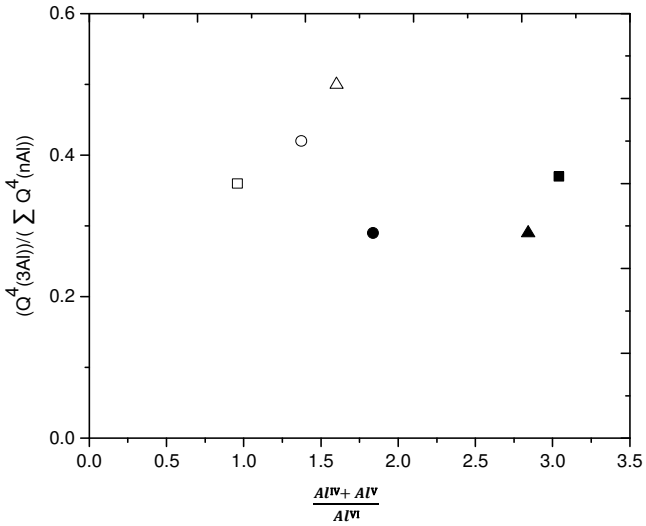

Figure 3: evolution of the contributions area ratio $\frac{Q^4(3Al)}{\sum Q^4(nAl)}$ of geopolymer samples GY and GY' in function of the $\frac{Al^{IV}+Al^{V}}{Al^{VI}}$ ratio of the raw mixtures (where GA (○), GB (Δ), GC (□) and GA' (●), GB' (▲), GC' (■)).

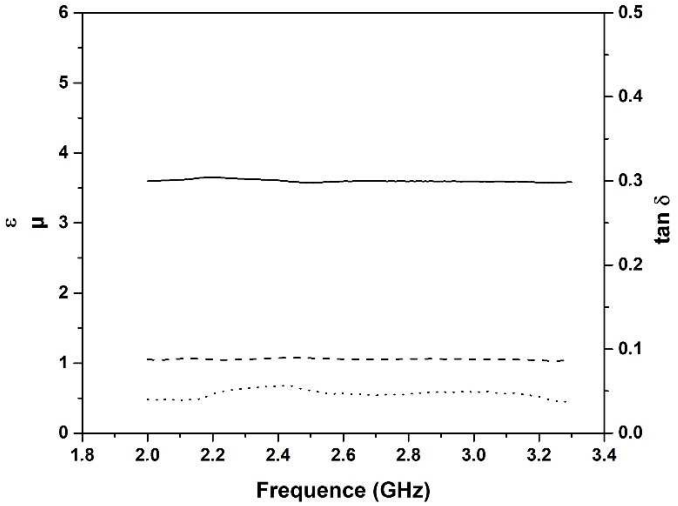

Figure 4: Frequency dependence of permittivity, loss tangent and permeability for GA sample (▬ ε; - - - μ; ···· tan δ).

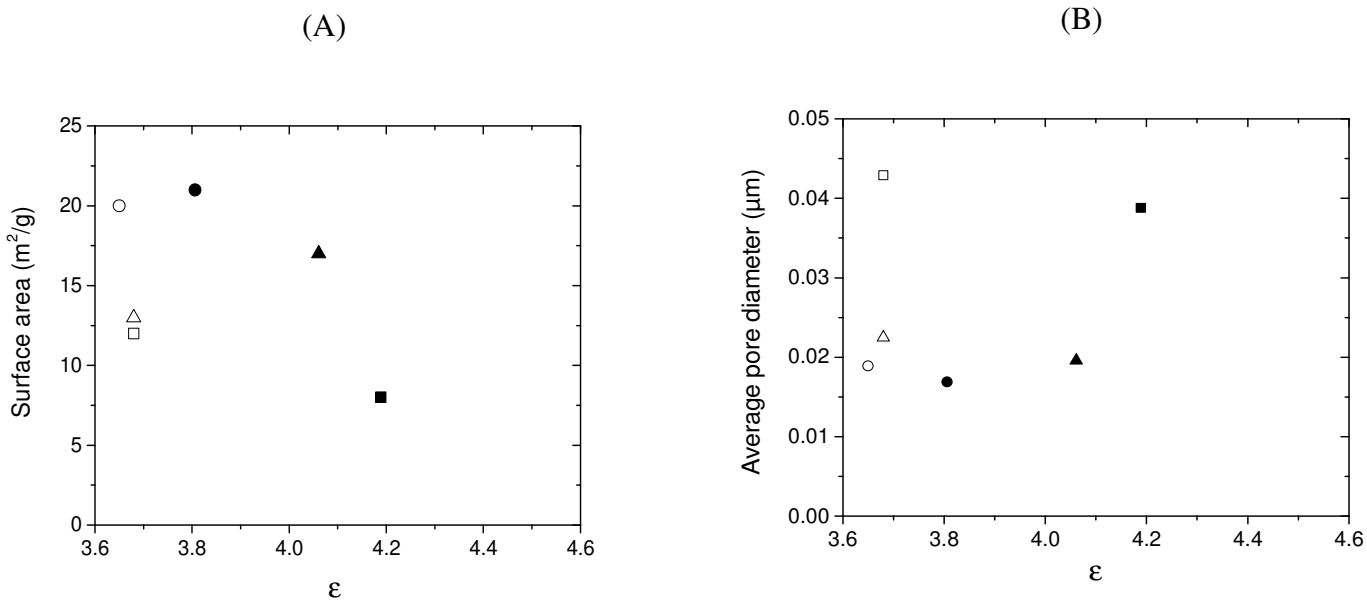

Figure 5 : **(A)** Value of surface area and **(B)** average pore diameter in function of ε value, for the geopolymer samples GY and GY' (where GA (○), GB (Δ), GC (□) and GA' (●), GB' (▲), GC' (■)).

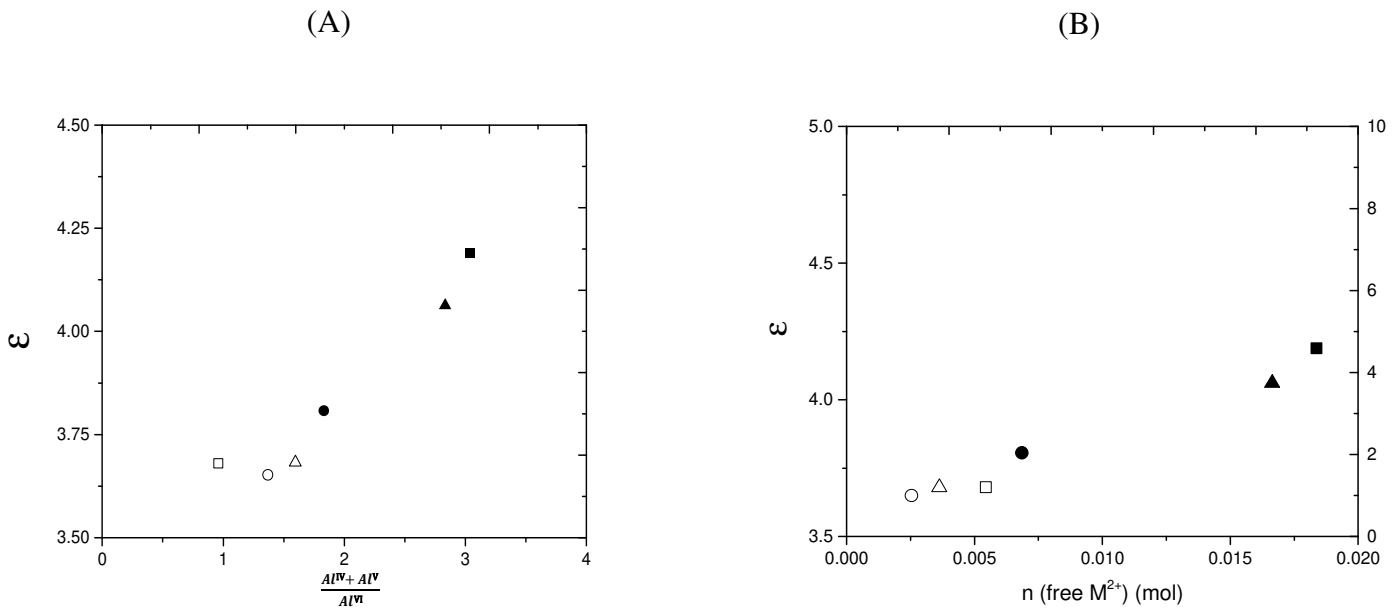

Figure 6 : Evolution of ε value of geopolymer samples GY and GY' in function of **(A)** the $\frac{Al^{IV}+Al^{V}}{Al^{VI}}$ ratio and **(B)** the number of moles of decomposed carbonates of the raw mixtures Y and Y' (where GA (○),GB (Δ),GC (□) and GA' (●), GB' (▲), GC' (■)).

Table 1. Nomenclature and chemical composition of the studied samples

Sample name	Calcination temperature (°C)	Argillite content (wt. %)	Molar ratios	
			Si/Al	Si/(K+H_2O)
GA	600	33	3.03	0.12
GB		50	3.60	0.17
GC		67	4.41	0.23
GA’	750	33	3.03	0.12
GB’		50	3.60	0.17
GC’		67	4.41	0.23

Table 2. Data from mercury porosimetry investigations for geopolymer samples GY and GY'

Sample	T, °C	Apparent density (g/cm^3)	Surface area (m^2/g)	Porosity (%)	Pore volume (mm^3/g)	Average pore diameter (µm)
GA	**600**	2.24	20	18	95	0.019
GB		2.23	13	14	75	0.023
GC		2.40	12	23	124	0.043
GA'	**750**	2.25	21	16	87	0.017
GB'		2.23	17	16	83	0.020
GC'		2.24	9	16	82	0.039

Table 3. Deconvolution details of ^{27}Al and ^{29}Si MAS-NMR spectra of the geopolymer samples GY and GY' and ^{27}Al MAS-NMR spectra of the raw mixtures Y and Y'.

Geopolymer samples									
Sample	^{27}Al MAS-NMR		^{29}Si MAS-NMR		Sample	^{27}Al MAS-NMR		^{29}Si MAS-NMR	
	δ (ppm)	Area (%)	δ (ppm)	Area (%)		δ(ppm)	Area (%)	δ (ppm)	Area (%)
GA	57.8	96.6	-75.0	2.8	GA'	58.0	97.8		
	2.5	3.4	-80.5	6.6		3.0	2.2	-81.7	18.5
			-85.0	23.5				-86.5	31.0
			-89.2	29.7				-90.1	22.4
			-93.4	21.0				-94.0	17.8
			-96.3	5.4					
			-99.5	8.6				-98.0	6.6
			-108	2.0				-107.5	3.6
GB	57.8	94.2	-78.0	3.4	GB'	58.2	97.7		
	3.0	5.9	-81.0	8.0		3.0	2.3	-81.7	19.5
			-85.0	21.5				-86.5	30.8
			-89.3	33.5				-90.1	22.7
			-94.5	22.9				-94.0	19.5
			-99.5	7.7				-99.0	4.9
			-107	2.9				-108.5	2.7
GC	58.0	91.3	-79.5	10.2	GC'	58.0	93.8	-78.0	5.9
	2.6	7.7	-84.0	18.9		3.0	6.3	-82.0	25.8
			-87.9	27.0				-86.5	31.3
			-92.2	29.3				-91.2	26.9
			-97.0	11.9				-97.0	6.7
			-107.9	2.7				-108.2	3.4

Raw mixtures (^{27}Al MAS-NMR)					
Sample	δ (ppm)	Area (%)	Sample	δ (ppm)	Area (%)
A	65.0	5.0	A'	64.5	3.6
	57.0	18.6		56.5	22.7
	48.5	2.9		48.5	3.9
	28.0	31.3		30	34.6
	13.5	6.4		13.5	8.53
	2.8	17.7		2.8	8.2
	-6.0	18.0		-6.0	18.5
B	65.00	8.5	B'	64.0	14.5
	56.2	22.7		56.5	21.9
	48.5	3.4		48.1	9.4
	28.5	27.0		30.0	29.6
	13.0	8.6		13.0	12.6
	3.2	13.9		3.2	6.1
	-6.0	16.0		-6.0	7.8
C	64.50	9.9	C'	63.5	17.3
	56.0	18.5		56.7	28.5

	48.5	4.9		48.5	10.4
	28.0	15.7		30.0	19.0
	12.5	7.9		13.0	14.8
	3.0	19.6		3.0	4.6
	-6.0	23.6		-6.0	5.4

Table 4. Values of ε, tan δ and μ for the geopolymer samples GY and GY' at 2.45 GHz, 20 °C and 45% humidity

Sample	T (°C)	Permittivity (ε)	Loss tangent (tan δ)	Permeability (μ)
GA	600	3.680	0.051	1.068
GB		3.694	0.038	1.040
GC		3.679	0.034	1.049
GA'	750	3.812	0.064	1.006
GB'		4.053	0.061	0.991
GC'		4.202	0.095	1.065

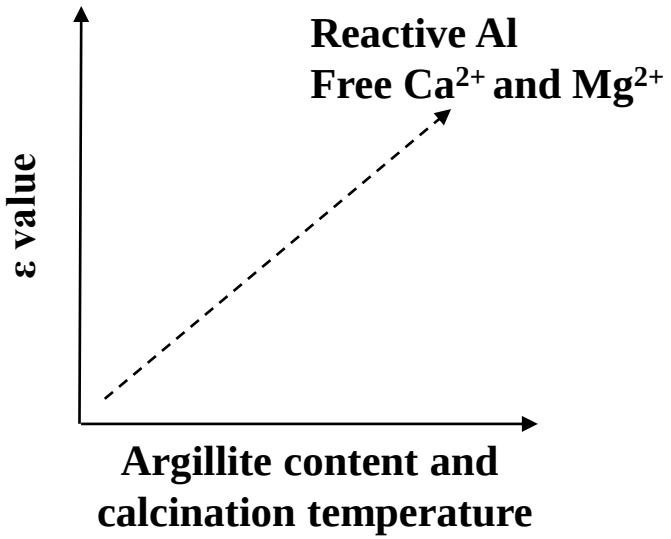
Reactive Al
Free Ca^{2+} and Mg^{2+}
ε value
Argillite content and
calcination temperature